Rhodamine–Ferrocene Conjugate Chemosensor for Selectively Sensing Copper(II) with Multisignals: Chromaticity, Fluorescence, and Electrochemistry and Its Application in Living Cell...

ARTICLE *in* ORGANOMETALLICS · MAY 2015

Impact Factor: 4.13 · DOI: 10.1021/acs.organomet.5b00285

4 AUTHORS, INCLUDING:

Yuan Fang
Nanjing Tech University, China
10 PUBLICATIONS **170** CITATIONS
SEE PROFILE

Yi Zhou
Nanyang Technological University
25 PUBLICATIONS **540** CITATIONS
SEE PROFILE

Cheng Yao
Nanjing Tech. University
111 PUBLICATIONS **746** CITATIONS
SEE PROFILE

ORGANOMETALLICS

Article

pubs.acs.org/Organometallics

Rhodamine–Ferrocene Conjugate Chemosensor for Selectively Sensing Copper(II) with Multisignals: Chromaticity, Fluorescence, and Electrochemistry and Its Application in Living Cell Imaging

Yuan Fang,[†] Yi Zhou,*[,†] Qingqing Rui,[†] and Cheng Yao*[,†,‡]

[†]State Key Laboratory of Materials-Oriented Chemical Engineering and College of Science, Nanjing Tech University, Nanjing 211816, People's Republic of China

[‡]State Key Laboratory of Coordination Chemistry, Nanjing University, Nanjing 210093, People's Republic of China

Supporting Information

ABSTRACT: A ferrocene unit is introduced into the salicylaldehyde Rhodamine 6G hydrazone with an alkynyl group to constitute a new chemosensor, **R6G-FC**, for specifically sensing Cu^{2+} over other metal ions with multisignals. Upon interaction with Cu^{2+} in aqueous solution, **R6G-FC** expresses a detectable fluorescence enhancement along with changes in UV–vis absorption spectra and electrochemical parameters due to the binding-induced spirolactam ring-opening process in Rhodamine 6G. The complexation process between **R6G-FC** and Cu^{2+} can be carried out within a wide pH range in a short response time and with a good reversibility. **R6G-FC** also exhibits an excellent performance in sensing Cu^{2+} in the "dip-stick" method with an evident color gradation, and confocal fluorescence microscopy imaging results reveal that **R6G-FC** can be used to visualize Cu^{2+} in living HeLa cells with low cytotoxicity.

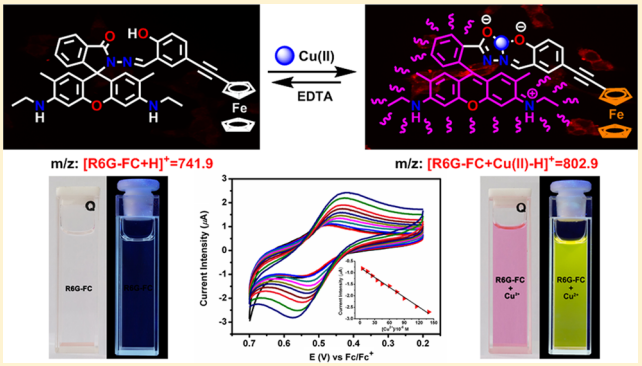

INTRODUCTION

Copper, which ranks third in abundance among the essential trace metal ions (after iron and zinc) in the human body, plays an important role in various environmental, chemical, and physiological systems.[1] There are many reactions in biological processes that involve electron transfer that are catalyzed by copper-containing enzymes.[2] Disturbing the concentration balance of intracellular Cu^{2+} may cause several neurological diseases, such as Menkes syndrome,[3] Wilson's disease,[3b,e,4] amyotrophic lateral sclerosis,[3e,5] Alzheimer's disease,[5b,d,6] and prion disorder.[5c,d,6c,d,7] Therefore, it is of great importance to accurately detect copper ions in the real environment, especially to strictly monitor and control the distribution of intracellular Cu^{2+}.

In the last few decades, many advanced analytical methods have been developed to both qualitatively and quantitatively determine Cu^{2+}, such as spectrophotometry,[8] atomic absorption spectroscopy,[9] inductively coupled plasma mass spectroscopy (ICP-MS),[10] inductively coupled plasma atomic emission spectrometry (ICP-AES),[11] and voltammetry.[12] Among them, owing to the high sensitivity, excellent selectivity, nondestructiveness, and low cost, novel fluorescent chemosensors have drawn a lot of attention in the area of analytical chemistry, especially in biological analysis. Cu^{2+}, with the $3d^9$ outermost electron structure, is known as a fluorescence quencher because of its paramagnetic property.[13] As a result, many of the reported fluorescent chemosensors detect Cu^{2+} through a fluorescence quenching process that undergoes an energy or electron transfer mechanism.[14] In the consideration of sensitivity, fluorescence enhancement (turn-on) signals are much easier to detect than fluorescence quenching (turn-off) ones. The rhodamine fluorophore, known for its excellent spectroscopic properties and good water solubility, is an ideal moiety to construct "turn-on"-type fluorescent chemosensors in terms of metal ions triggering the spirolactam ring-opening mechanism along with changes in chromaticity and fluorescence at the same time.[15,16] Considering the high affinity of Cu^{2+} to N and O atoms, rhodamine-hydrazone is an excellent platform to design novel fluorescent chemosensors for specifically sensing Cu^{2+} with high sensitivity in an aqueous solvent,[15h,m,16] even *in vivo*,[16] which has drawn a great deal of researchers' attention in recent years. On the other hand, as a traditional electrochemical signal donor, ferrocene has been widely applied in designing chemosensors for various cations and anions due to its good solubility and high biocompatibility.[17] When interacting with an analyte, ferrocene-based chemosensors usually express a significant potential shift of the Fe^{III}/Fe^{II} redox couple, which could be in combination with other signals to obtain a multichannel sensing event.[18,19] In

Received: April 4, 2015
Published: May 20, 2015

DOI: 10.1021/acs.organomet.5b00285
Organometallics 2015, 34, 2962–2970

comparison with traditional single-signal chemosensors, small-molecule scaffolds with the ability to generate multichannel signals (chromogenic, fluorogenic, and electrochemical) provide better selectivity, higher sensitivity, and self-calibration ability through variable detecting methods with low background in complex systems. The development of multichannel Cu^{2+}-selective chemosensors based on rhodamine–ferrocene, in particular, is a relatively unexplored area with only a very few examples being reported including one of our group's recent work (Table S1, Supporting Information).[20] Therefore, it is still in demand and meaningful to keep modifying the molecular structures and examining the sensing behavior between the new rhodamine–ferrocene multichannel chemosensors and Cu^{2+}. Inspired by the work of Tong,[21] we additionally introduced a ferrocene unit into a salicylaldehyde Rhodamine 6G hydrazone platform through an alkynyl to construct a novel multisignaling chemosensor, **R6G-FC** (Scheme 1), for selectively sensing Cu^{2+}

Scheme 1. Molecule Design of the Chemosensor R6G-FC

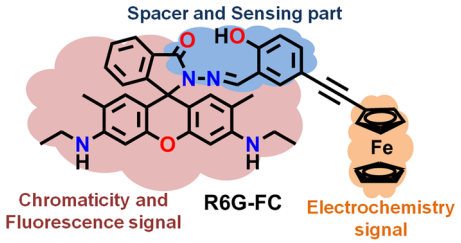

with colorimetric, fluormetric, and electrometric readouts (Table S2, Supporting Information). Moreover, with low cytotoxicity and good solubility, **R6G-FC** could be used as a fluorescent chemosensor to image Cu^{2+} in living HeLa cells.

EXPERIMENTAL SECTION

Instruments and Reagents. Chromatographic separation was done by column chromatography using 300–400 mesh silica gel. ^1H NMR and ^{13}C NMR were recorded on BrukerAV-500 and BrukerAV-400 spectrometers with chemical shifts reported in ppm (in $CDCl_3$; TMS as internal standard). Electrospray ionization mass spectra (ESI-MS) were analyzed on a Micromass LCTTM system and Thermo Finnigan LCQ Advantage spectrometer. Elemental analyses (C, H, and N) were carried out on a PerkinElmer 240C elemental analyzer. Melting points were determined on an XT4-100A hot-plate melting point apparatus and are uncorrected. All the pH measurements were monitored with a Sartorius PB-10 basic pH meter. UV–vis spectra and fluorescence spectra were recorded on a PerkinElmer Lambda 35 spectrometer and a PerkinElmer LS-50B fluorescence spectrophotometer at room temperature, respectively. Electrochemical measurements were conducted with a Shanghai CHI 660D electrochemical workstation. Fluorescence imaging was done with an Olympus BX51. The cytotoxicity assay was determined using an SLT Spectra Shell microplate reader spectrophotometer. Unless otherwise specified, materials were obtained from commercial suppliers and were used as received. All the solvents were of analytic grade, and water was redistilled. The salts used in stock solutions of metal ions were $NaNO_3$, KNO_3, $Mg(NO_3)_2{\cdot}6H_2O$, $Ca(NO_3)_2{\cdot}4H_2O$, $Al(NO_3){\cdot}9H_2O$, $Cr(NO_3)_3{\cdot}9H_2O$, $AgNO_3$, $Ba(NO_3)_2$, $Hg(NO_3)_2{\cdot}H_2O$, $Mn(NO_3)_2{\cdot}4H_2O$, $Pb(NO_3)_2$, $Cd(NO_3)_2{\cdot}4H_2O$, $Ni(NO_3)_2{\cdot}6H_2O$, $Zn(NO_3)_2{\cdot}6H_2O$, $Co(NO_3)_2{\cdot}6H_2O$, $Fe(NO_3)_3{\cdot}9H_2O$, and $Cu(NO_3)_2{\cdot}3H_2O$. Rhodamine 6G, ethynylferrocene, 5-bromosalicylaldehyde, $Pd(PPh_3)_2Cl_2$, and CuI were purchased from Alfa Aesar. The other reagents were purchased from Taiyuan RHF Reagents Co. Ltd.

Property Test Procedures. A stock solution (1.0×10^{-3} M) of **R6G-FC** was prepared in DMSO. Stock solutions (1.0×10^{-2} M) of the nitrate salts of Na^+, K^+, Mg^{2+}, Ca^{2+}, Al^{3+}, Cr^{3+}, Ag^+, Ba^{2+}, Hg^{2+}, Mn^{2+}, Pb^{2+}, Cd^{2+}, Ni^{2+}, Zn^{2+}, Co^{2+}, Fe^{3+}, and Cu^{2+} in water were prepared as well. Before spectral measurements, **R6G-FC** with different concentrations of Cu^{2+} was freshly prepared by diluting the high-concentration stock solution with $EtOH/H_2O$ (1:1, v/v, pH = 7.0) to the corresponding solution and shaken for 10 s. 5 and 20 min latency times were needed before UV–vis and fluorescence detection, respectively. Fluorescence measurements were carried out with a 500 nm excitation wavelength and 10 nm slit width. All electrochemical experiments were measured under a nitrogen atmosphere at room temperature in a one-compartment container equipped with a glassy-carbon working electrode, a platinum-wire auxiliary electrode, and an SCE reference electrode. The supported electrolyte was 50 mM tetrabutyl ammonium hexafluorophosphate ($(n\text{-}Bu)_4NPF_6$) in a solution of CH_3CN/H_2O (7:3, v/v, pH = 7.0). In selectivity experiments, one batch of sample was prepared by separately placing different kinds of metal ions into a stock solution of **R6G-FC** and then diluted with $EtOH/H_2O$ (1:1, v/v, pH = 7.0) to the target concentration of **R6G-FC** (10 μM). The other batch of sample was additionally prepared by adding a proper amount of Cu^{2+} into each of the latter samples. Ethylenediamine tetraacetic acid disodium salt (EDTA) was chosen as the chelating agent with Cu^{2+} to confirm the reversibility of the chemosensor **R6G-FC**. The wide pH range solutions were prepared by adjustment of pH buffer solutions with HCl or NaOH. In the "dip-stick" method, TLC plates were first immersed into an ethanol solution of **R6G-FC** (1×10^{-4} M) and then the solvent was evaporated to dryness. The modified TLC plates were separately dropped into different concentrations of Cu^{2+} (0, 1, 10, and 100 ppm) in distilled water and then dried in the dark in the air.

Cell Culture and Fluorescence Imaging. HeLa cells were cultured on a 24-well plate with a density of 2×10^3 cells per well in Dulbecco's modified Eagle medium (DMEM, Gibco) supplemented with 10% fetal bovine serum (FBS, Sigma), penicillin (100 $\mu g{\cdot}mL^{-1}$), and streptomycin (100 $\mu g{\cdot}mL^{-1}$) at 37 °C in a humidified atmosphere with 5% CO_2 and 95% air for 24 h prior to staining. After washing with PBS buffer (phosphate-buffered saline, pH = 7.2, Gibco), HeLa cells were then incubated with chemosensor **R6G-FC** (10 μM) and Hoechst 33342 (10 μM) in the culture media containing ethanol/PBS (1:49, v/v) for 30 min at 37 °C. To remove the remaining **R6G-FC**, cells were additionally washed with PBS buffer three times. Experiments to assess Cu(II) uptake were performed in the same culture media supplemented with 100 μM $Cu(NO_3)_2$ for 1 h. The treated HeLa cells were rinsed with PBS three times, and the fluorescence images were acquired through fluorescence microscopy (BX51, Olympus, Japan).

Cytotoxicity Assay. To investigate the cytotoxicity of the chemosensor **R6G-FC** in the cells over a 24 h period, a typical MTT (3-(4,5-dimethyl-2-thiazolyl)-2,5-diphenyl-2*H*-tetrazolium bromide) assay was performed. Before the treatment of cells with **R6G-FC**, HeLa cells under log phase growth were plated in 96-well plates (5×10^4 cells per well) overnight. Chemosensor **R6G-FC** with final concentrations of 1, 5, 25, 50, and 100 μM, which were diluted from the stock solution, was separately added to HeLa cells, and the treated cells were incubated at 37 °C under 5% CO_2 and 95% air for 24 h. After removing the medium and adding 20 μL of MTT solution (5 mg/mL, PBS), the HeLa cells were incubated for another 4 h at 37 °C under 5% CO_2 and 95% air. Then the solution was removed, and 150 μL of DMSO was added to the cells. After agitating on an orbital shaker for 10 min, the absorbance of each well at 570 nm was recorded. The other batch of cells was treated according to the above steps and incubated for 48 h before recording the absorbance. The cell viability (%) was calculated according to the following equation: cell viability (%) = $OD_{570(sample)}/OD_{570(control)} \times 100$, where $OD_{570(sample)}$ represents the optical densities of the wells treated with various concentrations of chemosensor **R6G-FC** and $OD_{570(control)}$ represents that of the wells treated with DMEM plus 10% FBS. The percentage cell survival values are relative to untreated control cells.

Synthesis of Rhodamine 6G Hydrazide (1). Rhodamine 6G hydrazide (**1**) was synthesized according to the reported method.[19c] ^1H NMR (500 MHz, $CDCl_3$): δ = 7.95 (d, J = 3.5 Hz, 1H, Ar–H), 7.45 (s, 2H, Ar–H), 7.06 (d, J = 3.5 Hz, 1H, Ar–H), 6.39 (s, 2H,

DOI: 10.1021/acs.organomet.5b00285
Organometallics 2015, 34, 2962–2970

Scheme 2. Synthetic Route of Chemosensor R6G-FC

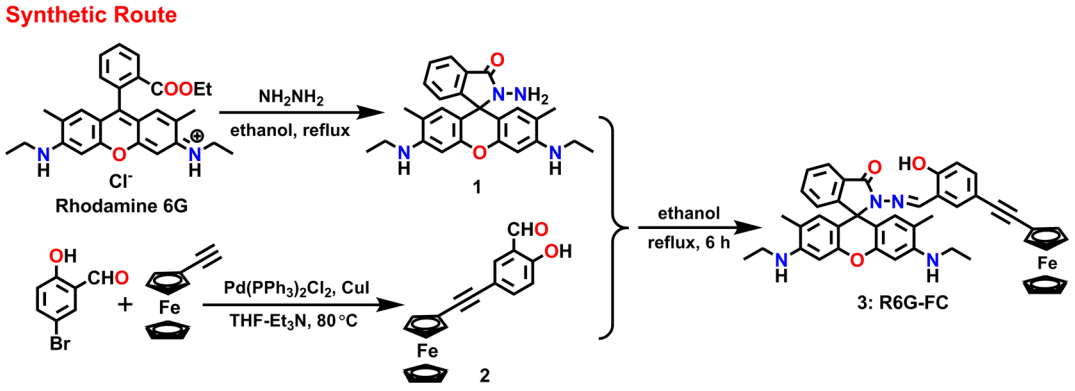

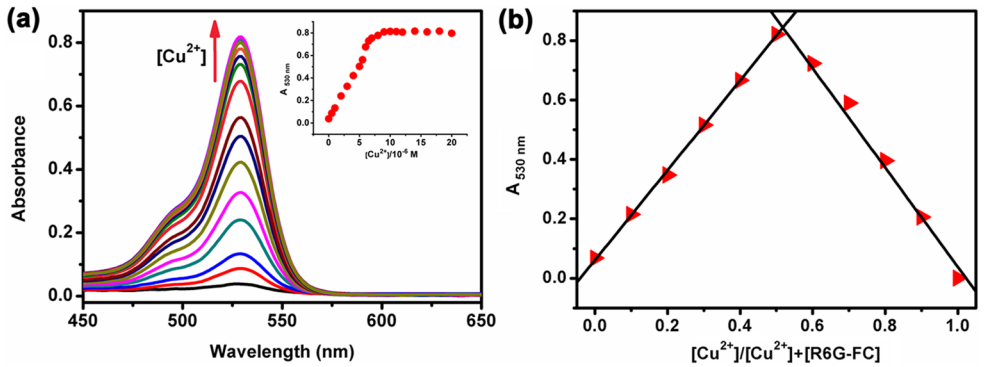

Figure 1. (a) UV−vis absorption spectra of **R6G-FC** (10 μM) upon addition of different amounts of Cu^{2+} (0−20 μM) in EtOH/H_2O (1:1, v/v, pH = 7.0). Inset: The value of UV−vis absorption at 530 nm as a function of Cu^{2+} concentrations. (b) Job's plot of chemosensor **R6G-FC** with Cu^{2+} ([**R6G-FC**] + [Cu^{2+}] = 20 μM). The detection wavelength was 530 nm.

xanthene−H), 6.26 (s, 2H, xanthene−H), 3.58 (s, 2H, $-NH_2$), 3.48 (br s, 2H, −NH−), 3.22 (q, J = 6.8 Hz, 4H, $-CH_2-$), 1.92 (s, 6H, Ar−CH_3), 1.32 (t, J = 6.6 Hz, 6H, $-CH_3$).

Synthesis of 5-Ethynylferrocene-salicylaldehyde (2). In a 250 mL flask, ethynylferrocene (7.5 mmol, 1.58 g), 5-bromosalicylaldehyde (5 mmol, 1.01 g), $Pd(PPh_3)_2Cl_2$ (0.5 mmol, 0.35 g), and CuI (0.12 mmol, 0.03 g) were all dissolved in a mixed solvent (160 mL) of THF/Et_3N (1:1, v/v), and the reaction mixture was refluxed at 80 °C overnight under a N_2 atmosphere. At the end of the reaction, the resulting ammonium salt was filtered off, and the amine solution was evaporated under reduced pressure. The crude product was purified by flash chromatography first with petroleum ether/CH_2Cl_2 (6:1, v/v) to remove low-polar impurities followed by an elution of petroleum ether/CH_2Cl_2 (3:1, v/v, R_f = 0.25). The fourth band was collected, and an orange solid **2** (0.67 g, yield: 40%) was afforded after removal of the solvent.[22] Mp: 164.9−165.3 °C. ^{1}H NMR (400 MHz, $CDCl_3$): δ = 11.07 (s, 1H, −OH), 9.89 (s, 1H, −CHO), 7.70 (d, J = 2.1 Hz, 1H, Ar−H), 7.62 (dd, J = 8.6, 2.1 Hz, 1H, Ar−H), 6.96 (d, J = 8.6 Hz, 1H, Ar−H), 4.49 (t, J = 1.8 Hz, 2H, Fc−H), 4.26 (s, 7H, Fc−H). ^{13}C NMR (101 MHz, $CDCl_3$): δ = 196.18, 160.98, 139.75, 136.57, 120.50, 118.02, 115.97, 87.88, 83.84, 71.38, 69.99, 68.92, 64.87. Anal. Calcd for $C_{19}H_{14}FeO_2$: C, 69.12; H, 4.27. Found: C, 69.05; H, 4.33. TOF-MS (negative ion mode): m/z 329.1 $[M - H]^+$, 330.1 $[M]^+$.

*Synthesis of Chemosensor **R6G-FC** (**3**).* Rhodamine 6G hydrazide (**1**) (1.0 mmol, 0.43 g) and 5-ethynylferrocene-salicylaldehyde (**2**) (1.5 mmol, 0.49 g) were dissolved in anhydrous ethanol (10 mL), and the mixture was heated at 60 °C for 12 h under a N_2 atmosphere. The resulting wine red mixture was filtered and washed with cold ethanol to afford an earthy red solid, which was then recrystallized from anhydrous ethanol to provide the pure final product **R6G-FC** (**3**) (0.43 g, 58%).[21] Mp: 235.2−236.0 °C. ^{1}H NMR (400 MHz, $CDCl_3$): δ = 11.22 (s, 1H, −OH,), 8.83 (s, 1H, N=C−H), 8.01 (d, J = 8.0 Hz, 1H, Ar−H), 7.52 (p, J = 7.6 Hz, 2H, Ar−H), 7.29 (d, J = 1.4 Hz, 1H, Ar−H), 7.16 (d, J = 1.3 Hz, 1H, Ar−H), 7.11 (dd, J = 4.0 Hz, 1H, Ar−H), 6.81 (d, J = 8.5 Hz, 1H, Ar−H), 6.44 (s, 2H, xanthene−H), 6.30 (s, 2H, xanthene−H), 4.45 (s, 2H, Fc−H), 4.21 (d, J = 4.8 Hz, 7H, Fc−H), 3.55−3.47 (m, 2H, −NH−), 3.22 (d, J = 6.7 Hz, 4H, $-CH_2-$), 1.89 (s, 6H, Ar−CH_3), 1.32 (t, J = 7.1 Hz, 6H, $-CH_3$). ^{13}C NMR (101 MHz, $CDCl_3$): δ 164.45, 158.32, 151.64, 151.55, 150.18, 147.80, 134.22, 133.74, 129.01, 128.57, 127.67, 124.02, 123.46, 118.55, 118.20, 117.35, 114.37, 107.70, 105.35, 96.82, 86.47, 85.07, 71.24, 69.91, 68.63, 65.58, 38.34, 16.76, 14.74. Anal. Calcd for $C_{45}H_{40}FeN_4O_3$: C, 72.97; H, 5.44; N, 7.56. Found: C, 73.05; H, 5.50; N, 7.49. TOF-MS: m/z 741.9 $[M + H]^+$.

RESULTS AND DISCUSSION

Synthesis and Characterization. Chemosensor **R6G-FC** is a Schiff base synthesized according to Scheme 2. Ethynylferrocene first reacted with 5-bromosalicylaldehyde through a Sonogashira coupling reaction and then was connected with Rhodamine 6G hydrazone to afford the target product **R6G-FC** as an earthy red solid with a yield of 58%. In the structure of **R6G-FC**, the Rhodamine 6G fluorophore acts as a colorimetric and fluorescent signal donor, and the ferrocene moiety provides an electrochemical signal with salicylaldeheyde and the Schiff base as the spacer and sensing part. **R6G-FC** is stable in its DMSO stock solution (1.0×10^{-3} M) for over 2 weeks. The sensing behavior of **R6G-FC** with Cu^{2+} was preliminarily tested in several common solvents (ethanol, water, acetonitrile, methanol, dimethyl sulfoxide), which were used for spectral detection. As depicted in Figure S8 (Supporting Information), except for dimethyl sulfoxide quenching the fluorescence of the ring-opened form of Rhodamine 6G, **R6G-FC** in the five different solvents could all give signal responses to Cu^{2+} in varying degrees. Ethanol

DOI: 10.1021/acs.organomet.5b00285
Organometallics 2015, 34, 2962−2970

solution of **R6G-FC** gave the best signal response to Cu^{2+} in both UV−vis absorption and fluorescence emission spectra compared to the other four solvents. Considering the intensity of the signal and the toxicity of the solvent, the ethanol−water mixed solvent (1:1, v/v) was chosen as the spectral test solution of **R6G-FC** for sensing Cu^{2+}. The time dependence experiment of **R6G-FC** after adding Cu^{2+} was investigated with both the UV−vis absorption and fluorescence emission method, and the signals remained stable after 5 and 20 min, respectively (Figure S9, Supporting Information).

UV−Visible Absorption Studies. The UV−vis spectral properties of **R6G-FC** were examined through a titration experiment (Figure 1a). The initial state of **R6G-FC** exhibited almost no absorption from 450 to 650 nm, indicating that most of the **R6G-FC** molecules stayed in the ring-closed spirolactam form. With the addition of Cu^{2+}, a new absorption peak emerged at 530 nm, which was in accordance with the typical absorption wavelength of ring-open Rhodamine 6G. The intensity of absorption increased along with the increasing concentration of Cu^{2+} (0−0.55 equiv) in a good linear relationship (R^2 = 0.9990, Figure S10, Supporting Information). After titrating approximately 1 equiv of Cu^{2+} into the system of **R6G-FC**, the intensity of absorption at 530 nm no longer increased to afford the **R6G-FC**/Cu^{2+} complex with the mole absorption coefficient ε of 8.16×10^4 $L \cdot mol^{-1} \cdot cm^{-1}$, suggesting the completed formation of spirolactam ring-opened **R6G-FC**. Additionally, the ratio relationship between **R6G-FC** and Cu^{2+} was estimated with a Job's plot experiment. From Figure 1b, it could be seen that the maximum value of absorption appeared at 0.5, which indicated that the stoichiometry of the **R6G-FC**/Cu^{2+} complex was 1:1. According to the UV−vis titration experiment, the value of $1/(A - A_0)$ of **R6G-FC** at 530 nm versus $1/[Cu^{2+}]$ also had a good linear relationship with R^2 = 0.9960, which was consistent with the Job's plot result (Figure S11, Supporting Information). Hence, the association constant K_a of **R6G-FC**/Cu^{2+} could be calculated based on the revised Benesi−Hildebrand equation as 1.52×10^6 M^{-1} (error <10%) (eq 1, Supporting Information).[23]

Fluorescence Emission Studies. In the investigation of the fluorescence property of **R6G-FC** (Figure 2), only weak fluorescence of the individual **R6G-FC** system was observed due to the main existing form of the spirolactam structure in **R6G-FC**. When Cu^{2+} was added to the system, the fluorescence emission centered at 554 nm gradually increased along with the increasing amount of Cu^{2+}, indicating that the ring-opened form of **R6G-FC** became the predominant species to release the fluorescence of Rhodamine 6G. Furthermore, the fluorescent color of the solution of **R6G-FC** changed significantly after interaction with Cu^{2+} from dark to bright yellow by naked-eye observations under UV light (365 nm) (Figure 2b). The values of fluorescence intensity were proportional to the concentration of Cu^{2+} within two ranges, 0.5−8.0 and 8.0−15 μM, respectively, and with a good linear relationship (Figure S12, Supporting Information). Also, the detection limit (S/N = 3) of **R6G-FC** to Cu^{2+} was determined to be 6.97×10^{-7} M (Figure S13, Supporting Information).[24] The fluorescence turn-on response of **R6G-FC** was in good agreement with the results of the UV−vis titration studies, which demonstrated that **R6G-FC** was a qualitative and quantitative chemosensor for Cu^{2+} in aqueous solution.

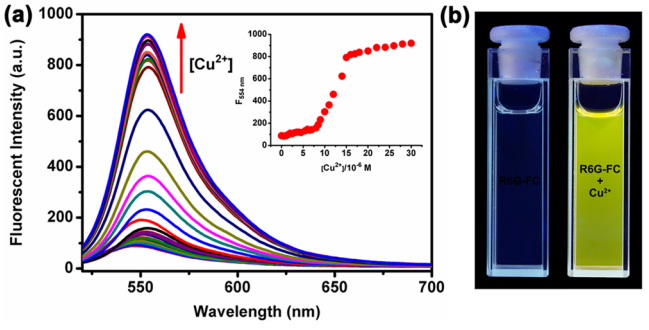

Figure 2. (a) Fluorescence emission spectra of **R6G-FC** (10 μM) in the presence of different concentrations of Cu^{2+} (0−32 μM) in EtOH/H_2O (1:1, v/v, pH = 7.0). Inset: The value of fluorescent intensity at 554 nm as a function of Cu^{2+} concentrations. Excitation wavelength was 500 nm. (b) Image of fluorescence change of **R6G-NA** (10 μM) before (left) and after (right) interaction with Cu^{2+} (30 μM).

Selectivity Studies. The signal response of **R6G-FC** toward various metal ions, such as Na^+, K^+, Mg^{2+}, Ca^{2+}, Al^{3+}, Cr^{3+}, Ag^+, Ba^{2+}, Hg^{2+}, Mn^{2+}, Pb^{2+}, Cd^{2+}, Ni^{2+}, Zn^{2+}, Co^{2+}, and Fe^{2+}, was also studied with both UV−vis absorption and fluorescence emission spectroscopy under the identical conditions of Cu^{2+} (Figure 3). Compared to the remarkable enhancement of absorption intensity of **R6G-FC** induced by Cu^{2+}, the influence caused by other metal ions was negligible even at the millimolar level (alkali and alkali-earth metal ions) in addition to the slight absorption enhancement brought by Fe^{2+}.[21] Consistent with the absorption enhancement, the color of the **R6G-FC** system obviously changed from colorless to pink after adding Cu^{2+}, which could be observed by the naked-eye (Figure 3a). To further explore the selectivity of **R6G-FC** to Cu^{2+}, a competition experiment was conducted by additionally mixing Cu^{2+} with an **R6G-FC** solution in the presence of other metal ions (Figure 3b). The bar graph of the fluorescence emission intensity revealed that the Cu^{2+}-triggered fluorescence enhancement of **R6G-FC** almost remained unaffected in the presence of higher concentrations of other metal ions. Hence, the above results of the optical experiments all indicated that **R6G-FC** had a high sensitivity and selectivity toward Cu^{2+} with no interference from other metal ions even at higher concentrations, thus revealing that **R6G-FC** could be assumed to be a Cu^{2+}-selective chemosensor.

Electrochemical Studies. The electrochemical signal, which can be easily read out on-site, is another essential parameter for ferrocene-containing chemosensors in the recognition process.[25] After introducing Cu^{2+} into the chemosensor system, the triggered ring-opening process of the spirolactam in **R6G-FC** would induce a change in the molecular configuration and then influence the electron density within the ferrocene group to express distinct electrochemical signals. The cyclic voltammetry (CV) and differential pulse voltammetry (DPV) experiment of the Cu^{2+}-recognition properties of **R6G-FC** were conducted in an aqueous CH_3CN solution with (n-Bu)$_4NPF_6$ (50 mM) as supporting electrolyte. Free **R6G-FC** displayed a reversible one-electron oxidation process at 0.508 V ($\Delta E_{1/2}$ = 62 mV) in the cyclic voltammogram, corresponding to the ferrocene/ferrocenium redox couple (Figure 4a).[26] Upon stepwise addition of Cu^{2+} (0−2.8 equiv), the original peak gradually evolved to 0.495 V ($\Delta E_{1/2}$ = 140 mV), associated with the formation of the Cu^{2+}/**R6G-FC** complexed species. Meanwhile, the value of the current intensity of the oxidation peak had a good linear relationship with the concentration of Cu^{2+} added (inset in Figure 4a), which could be used to

DOI: 10.1021/acs.organomet.5b00285
Organometallics 2015, 34, 2962−2970

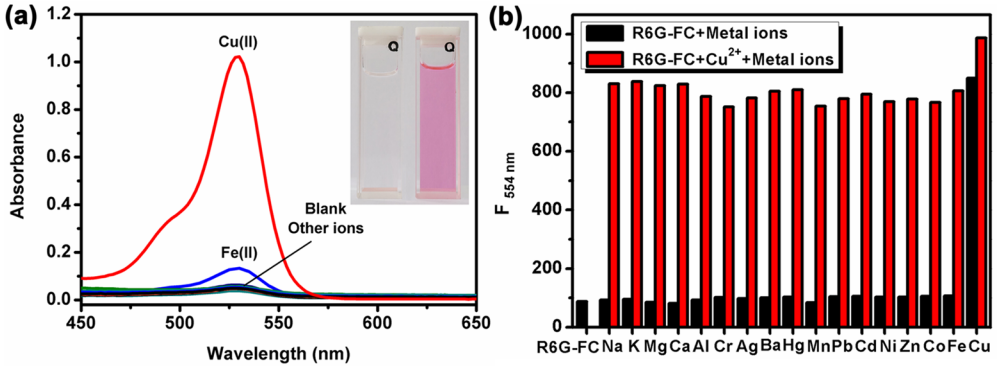

Figure 3. (a) UV−vis absorption spectra of **R6G-FC** (10 μM) in EtOH/H_2O (1:1, v/v, pH = 7.0) in the presence of different metal ions (1 mM for alkali and alkali-earth metal ions and 20 μM for transition metal ions): Na^+, K^+, Mg^{2+}, Ca^{2+}, Al^{3+}, Cr^{3+}, Ag^+, Ba^{2+}, Hg^{2+}, Mn^{2+}, Pb^{2+}, Cd^{2+}, Ni^{2+}, Zn^{2+}, Co^{2+}, Fe^{2+}, Cu^{2+}, and blank. Inset: Color changes of **R6G-FC** (10 μM) before (left) and after (right) addition of Cu^{2+} (2 equiv). (b) Fluorescence responses of 10 μM **R6G-FC** to various 20 μM transition metal ions (1 mM for alkali and alkali-earth metal ions). Spectra were acquired in EtOH/H_2O (1:1, v/v, pH = 7.0) with a 500 nm excitation wavelength. Bars represent the final fluorescent intensity at 554 nm. The black bars represent the fluorescence emission of a 10 μM **R6G-FC** solution with different competing metal ions. The red bars represent the change of the emission intensity that occurred on subsequent addition of 20 μM Cu^{2+} to the above solutions.

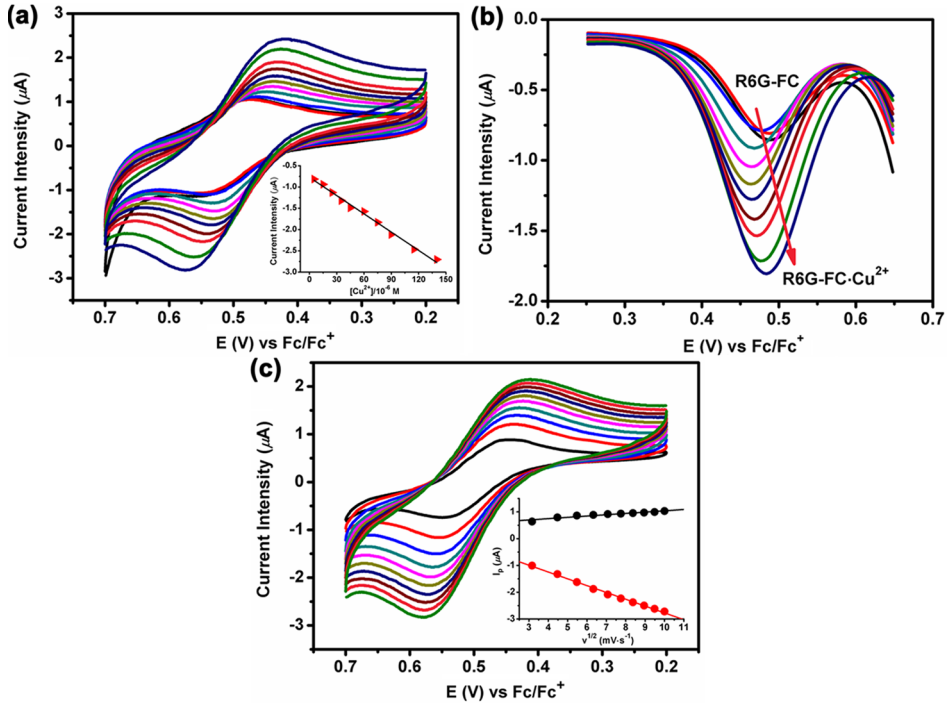

Figure 4. (a) CV of free **R6G-FC** (black) (50 μM) in CH_3CN/H_2O (7:3, v/v, pH = 7.0) and after adding different amounts of Cu^{2+} (0−140 μM). Initial electric potential was 0.2 V. Inset: Plot of the currents of the oxidation peak in the CV (scan rate is 100 mV/s) of free **R6G-FC** (50 μM) upon the addition of Cu^{2+} (0−140 μM). (b) DPV (200 ms pulse width) of free **R6G-FC** (black) (50 μM) upon the addition of Cu^{2+} (0−140 μM) in CH_3CN/H_2O (7:3, v/v, pH = 7.0), showing the changes of the peak potentials. (c) The family of CV curves of the **R6G-FC**-Cu^{2+} complexation species showing the changes of the current with the scan rate. Inset: Plots of anodic and cathodic peak currents versus the square root of the scan rates, $\nu^{1/2}$. $(n\text{-Bu})_4NPF_6$ (50 mM) was used as supporting electrolyte at 25 °C.

quantitatively detect Cu^{2+} at the micromole level with a detection limit of approximately 3 μM (Figure S14, Supporting Information), whereas almost no deviation of the CV curves of **R6G-FC** was observed in the presence of other metal cations, such as Na^+, K^+, Mg^{2+}, Ca^{2+}, Al^{3+}, Cr^{3+}, Ag^+, Ba^{2+}, Pb^{2+}, Cd^{2+}, Ni^{2+}, Zn^{2+}, Co^{2+}, and Fe^{2+} as their nitrate salts. The DPV curve of **R6G-FC** further illustrated the similarity of the results to those obtained from CV with a slight anodic shift and the decrease of the current intensity upon increasing the concentration of Cu^{2+} in aqueous solution, which might be caused by the slow diffusion of **R6G-FC** to the electrode after the interaction with Cu^{2+} (Figure 4b).[27] The reversibility of the Fc/Fc^+ redox couple of the chemosensor **R6G-FC** in the presence of 2.8 equiv of Cu^{2+} was confirmed by the linear relation between the peak currents and the square root of the scan rates (inset in Figure 4c), the small difference between anodic and cathodic peak currents, and the small peak-to-peak potential separations.[19c,d,20a]

Mechanism Studies of R6G-FC/Cu^{2+} Complexation. The reversibility of the sensing progress between **R6G-FC** and Cu^{2+} was examined with the EDTA-adding experiment (Figure S15, Supporting Information).[21,28] The spectral data revealed

DOI: 10.1021/acs.organomet.5b00285
Organometallics 2015, 34, 2962−2970

Scheme 3. Proposed Coordination Mechanism of R6G-FC with Cu^{2+}

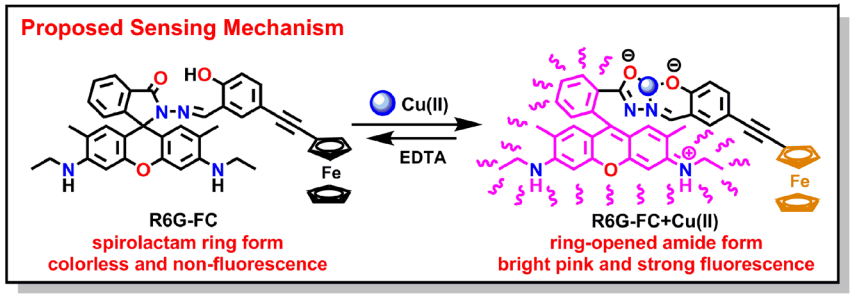

that adding 1 equiv of EDTA to the **R6G-FC**/Cu^{2+} system could restore the "on state" back to the "off state" in both absorption and fluorescence signals. Moreover, adding extra Cu^{2+} to the system could once again turn on the signals, which proved the sensing progress was reversible. Considering the spectral changes investigated above and the 1:1 binding stoichiometry confirmed by the Job's plot, the sensing mechanism between **R6G-FC** and Cu^{2+} could be speculated as in Scheme 3. Cu^{2+} first entered into the cave in the structure of **R6G-FC** and then coordinated with carbonyl O, imino N, and phenol O atoms, which would trigger the spirolactam of **R6G-FC** to open accompanied with a color change from colorless to pink and the fluorescence of Rhodamine 6G turning on as well. After the complexation, the electronic density within the ferrocene moiety was influenced by the Cu^{2+}-binding-induced electron portion of the Rhodamine 6G moiety, which would consequently cause a significant shift of the redox potential of the ferrocenyl group. In addition, the proposed sensing mechanism between **R6G-FC** and Cu^{2+} was then confirmed with the TOF-MS results with the appearance of a new ion peak of m/z 802.9, which indicated the formation of $[$**R6G-FC**+Cu(II)-H$]^+$ (calcd 803.2) (Figure S16, Supporting Information).

R6G-FC Performance in Pure Water and Dip-Stick Studies. In order to demonstrate practical applications of this new chemosensor, **R6G-FC** was used to judge the existence of Cu^{2+} in a pure water system (Figure 5a). The color of the **R6G-FC** aqueous solution (10 μM) changed from colorless to light pink even when only 0.5 ppm of Cu^{2+} was present, which identified that **R6G-FC** could serve as a diagnostic kit for trace amounts of Cu^{2+} in water. In addition, an easy "dip-stick" experiment with TLC plates bearing **R6G-FC** was performed to sense Cu^{2+} in pure water as well. Figure 5b presents the distinct color changes of TLC plates before and after being immersed into Cu(II)-containing water with different concentrations. Through this real-time monitoring method, it was possible to *in situ* detect Cu^{2+} at ppm levels in water without any help from analytical instruments. According to the U.S. Environmental Protection Agency (EPA), the limit of Cu^{2+} in drinking water is 1.3 ppm (~20 μM), which could be adequately detected with the chemosensor **R6G-FC** by the naked-eye inspection in both solution and TLC plates.[29]

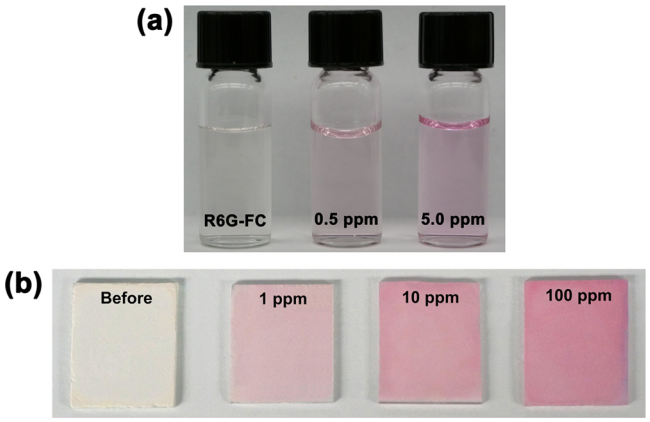

Figure 5. (a) Color changes of **R6G-FC** (10 μM) in aqueous solutions in the presence of Cu^{2+} with concentrations of 0, 0.5, and 5 ppm. (b) Thin-layer chromatography of **R6G-FC** before and after immersing in 1, 10, and 100 ppm of Cu^{2+} in distilled water, respectively.

Fluorescence Imaging Studies. The pH dependence experiment revealed that the fluorescence intensity of both **R6G-FC** and **R6G-FC**/Cu^{2+} could remain stable in a wide pH range from 5.0 to 10.5 (Figure S17, Supporting Information), inferring that **R6G-FC** could be applied to monitor Cu^{2+} under physiological conditions. Therefore, HeLa cells were chosen as the living model to investigate the capability of **R6G-FC** to fluorescence bioimaging Cu^{2+}. Initially, HeLa cells were cultured with only **R6G-FC** (10 μM) at 37 °C for 30 min, and almost no fluorescence was captured intracellularly by confocal fluorescence microscopy (Figure 6a). However, after adding 100 μM Cu^{2+} to the HeLa cells and then incubating for one more hour, remarkable red fluorescence was detected, which was consistent with the fluorescence turn-on mechanism of **R6G-FC** in the presence of Cu^{2+} in the solution (Figure 6d). Moreover, Hoechst 33342, a well-known cell nucleus staining reagent, was additionally used to show that **R6G-FC** had low cytotoxicity to the cells (Figure 6b,e). The overlay image also shows that the areas of red fluorescence and blue fluorescence complement each other and revealed that Cu^{2+} predominantly exists in the cytoplasmic part of the HeLa cells (Figure 6f). The results established that **R6G-FC** had good cell-membrane permeability and could be used in visualizing Cu^{2+} in living cells and potentially *in vivo*.

MTT Assay Studies. The MTT assay was conducted to further inspect the cytotoxicity of **R6G-FC** to the HeLa cell line when applied in bioapplications (Figure S18, Supporting Information). The HeLa cells were treated with 1, 5, 25, 50, and 100 μM **R6G-FC** and cultured for 24 and 48 h, respectively. Over the entire concentration range of **R6G-FC** employed in the experiment, after a 24 h incubation time, HeLa cell viability of the control remained above 80%. As for the low concentrations of **R6G-FC** (1−25 μM), a decrease of less than 15% in cell viability could still be observed, contrasting with the control group, even after 48 h of incubation time. Therefore, the concentration of **R6G-FC** (10 μM) used to acquire the confocal fluorescence images in Figure 6 was in the low concentration range and confirmed the low cytoxicity to HeLa

DOI: 10.1021/acs.organomet.5b00285
Organometallics 2015, 34, 2962−2970

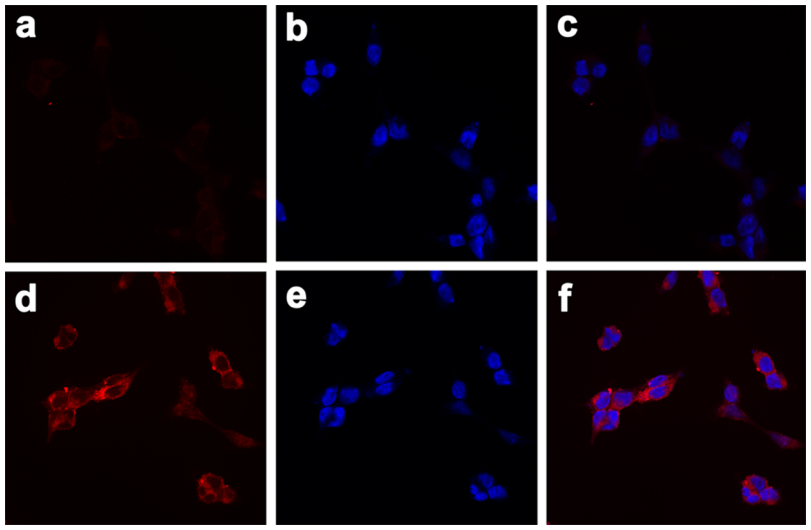

Figure 6. Confocal fluorescence images of **R6G-FC** in living HeLa cells. (a) Cells incubated with **R6G-FC** (10 μM) in ethanol/PBS (1:49, v/v) buffer for 30 min at 37 °C from the red channel. (b) Cell nucleus labeled with Hoechst 33342 (10 μM) for 30 min from the blue channel. (c) Overlay image of (a) and (b). (d) Cells pretreated with **R6G-FC** (10 μM) for 30 min, then incubated with Cu^{2+} (100 μM) for 1 h from the red channel. (e) Cells pretreated with **R6G-FC** (10 μM) and Hoechst 33342 (10 μM) for 30 min, then incubated with Cu^{2+} (100 μM) for 1 h from the blue channel. (f) Overlay image of (d) and (e).

cells, indicating that it would be suitable for this concentration of **R6G-FC** to be applied in cellular imaging studies.

CONCLUSION

In summary, a novel multisignaling chemosensor, **R6G-FC**, was designed and synthesized through the classic Sonogashira coupling reaction to introduce a ferrocenyl moiety into a modified Rhodamine 6G fluorophore. The addition of Cu^{2+} to an **R6G-FC** aqueous solution would result in a new UV−vis absorption peak and fluorescence emission peak in the optical spectrum, which was due to the binding-induced spirolactam ring opening of **R6G-FC**. Due to the high affinity of Cu^{2+} with N and O atoms, **R6G-FC** had good selectivity and high sensitivity to Cu^{2+} without interference from other metal ions. The detection limit obtained from fluorescence titration was down to 6.96×10^{-7} M, and the association constant was calculated from absorbance titration as 1.52×10^{6} M^{-1}. In addition, the molecular configuration change of **R6G-FC** after interaction with Cu^{2+} influenced the electronic density within the ferrocene group to express perturbation of the electrochemical parameters, and the value of the current intensity of the oxidation peak had a good linear relationship with the added concentration of Cu^{2+}, which could be another quantitative basis for detecting Cu^{2+} with a detection limit of approximately 3 μM. The response of **R6G-FC** to Cu^{2+} could be accomplished within a short time, with a good reversibility, in a wide pH range. The 1:1 binding mechanism between **R6G-FC** and Cu^{2+} was confirmed by the Job's plot experiment and TOF-MS result. The "dip-stick" experiment showed an evident color gradation, which illustrated that the chemosensor **R6G-FC** could act as a naked-eye detection approach to sense Cu^{2+}. Moreover, due to the good solubility and biocompatibility, **R6G-FC** could be used for the fluorescence imaging of Cu^{2+} in living HeLa cells with low cytotoxicity.

ASSOCIATED CONTENT

Supporting Information

Reported structures of multisignal chemosensors for sensing Cu^{2+}. Comparison of rhodamine-based systems with or without a neighboring ferrocene moiety around the phenol group. ^{1}H NMR, ^{13}C NMR, and mass spectra as characterization data of intermediates, final product **R6G-FC**, and **R6G-FC**/Cu^{2+} complex. Solvent, reversibility, time, and pH dependence curve. Response of UV−vis absorption, fluorescence emission, and oxidation peak currents to the increasing amounts of Cu^{2+}. Calculation of association constant and detection limit. Cytotoxicity assay by the MTT test. The Supporting Information is available free of charge on the ACS Publications website at DOI: 10.1021/acs.organomet.5b00285.

AUTHOR INFORMATION

Corresponding Authors

*Tel: +86-25-5813-9482. Fax: +86-25-5813-9482. E-mail: zhouyi624@126.com (Y. Zhou).

*E-mail: yaocheng@njtech.edu.cn; yaochengnjut@126.com (C. Yao).

Notes

The authors declare no competing financial interest.

ACKNOWLEDGMENTS

This work is supported by the Open Fund of the State Key Laboratory of Materials-Oriented Chemical Engineering (KL13-07), the Open Fund of the State Key Laboratory of Coordination Chemistry, the Postgraduate Education and Innovation Project of Jiangsu Province (KYLX_0772), the Specialized Research Fund for the Doctoral Program of Higher Education (20123221110012), and the China Postdoctoral Science Foundation (2014M550287).

REFERENCES

(1) (a) Cowan, J. A. *Inorganic Biochemistry: An Introduction*; John Wiley & Sons: New York, 1997. (b) Uauy, R.; Olivares, M.; Gonzalez, M. *Am. J. Clin. Nutr.* **1998**, *67*, 952S−959S. (c) Barceloux, D. G. *J.*

DOI: 10.1021/acs.organomet.5b00285
Organometallics 2015, 34, 2962−2970

Toxicol., Clin. Toxicol. **1999**, *37*, 217−230. (d) Tapiero, H.; Townsend, D. M.; Tew, K. D. *Biomed. Pharmacother.* **2003**, *57*, 386−398. (e) Kozlowski, H.; Janicka-Klos, A.; Brasun, J.; Gaggelli, E.; Valensin, D.; Valensin, G. *Coord. Chem. Rev.* **2009**, *253*, 2665−2685. (f) Jaiser, S. R.; Winston, G. P. *J. Neurol.* **2010**, *257*, 869−881.

(2) (a) Bertini, I.; Gray, H. B.; Lippard, S. J.; Valentine, J. S. *Bioinorganic Chemistry*; University Science Books: Mill Valley, CA, 1994. (b) Koval, I. A.; Gamez, P.; Belle, C.; Selmeczi, K.; Reedijk, J. *Chem. Soc. Rev.* **2006**, *35*, 814−840. (c) Que, E. L.; Domaille, D. W.; Chang, C. J. *Chem. Rev.* **2008**, *108*, 1517−1549.

(3) (a) Vulpe, C.; Levinson, B.; Whitney, S.; Packman, S.; Gitschier, J. *Nat. Genet.* **1993**, *3*, 7−13. (b) Bull, P. C.; Thomas, G. R.; Rommens, J. M.; Forbes, J. R.; Cox, D. W. *Nat. Genet.* **1993**, *5*, 327−337. (c) Waggoner, D. J.; Bartnikas, T. B.; Gitlin, J. D. *Neurobiol. Dis.* **1999**, *6*, 221−230. (d) Lutsenko, S.; Gupta, A.; Burkhead, J. L.; Zuzel, V. *Arch. Biochem. Biophys.* **2008**, *476*, 22−32. (e) Kim, B. E.; Nevitt, T.; Thiele, D. J. *Nat. Chem. Biol.* **2008**, *4*, 176−185.

(4) Zhang, L. M.; Lichtmannegger, J.; Summer, K. H.; Webb, S.; Pickering, I. J.; George, G. N. *Biochemistry* **2009**, *48*, 891−897.

(5) (a) Valentine, J. S.; Hart, P. J. *Natl. Acad. Sci. U.S.A.* **2003**, *100*, 3617−3622. (b) Barnham, K. J.; Masters, C. L.; Bush, A. I. *Nat. Rev. Drug Discovery* **2004**, *3*, 205−214. (c) Gaggelli, E.; Kozlowski, H.; Valensin, D.; Valensin, G. *Chem. Rev.* **2006**, *106*, 1995−2044. (d) Crichton, R. R.; Dexter, D. T.; Ward, R. J. *Coord. Chem. Rev.* **2008**, *252*, 1189−1199.

(6) (a) Multhaup, G.; Schlicksupp, A.; Hesse, L.; Beher, D.; Ruppert, T.; Masters, C. L.; Beyreuther, K. *Science* **1996**, *271*, 1406−1409. (b) Barnham, K. J.; Bush, A. I. *Curr. Opin. Chem. Biol.* **2008**, *12*, 222−228. (c) Brown, D. R.; Kozlowski, H. *Dalton Trans.* **2004**, 1907−1917. (d) Kozlowski, H.; Luczkowski, M.; Remelli, M.; Valensin, D. *Coord. Chem. Rev.* **2012**, *256*, 2129−2141.

(7) Millhauser, G. L. *Acc. Chem. Res.* **2004**, *37*, 79−85.

(8) (a) Pinto, J. J.; Moreno, C.; García-Vargas, M. *Talanta* **2004**, *64*, 562−565. (b) Fu, D. Y.; Yuan, D. *Spectrochim. Acta, Part A* **2007**, *66*, 434−437.

(9) (a) Pourreza, N.; Hoveizavi, R. *Anal. Chim. Acta* **2005**, *549*, 124−128. (b) Gonzáles, A. P. S.; Firmino, M. A.; Nomura, C. S.; Rocha, F. R. P.; Oliveira, P. V.; Gaubeur, I. *Anal. Chim. Acta* **2009**, *636*, 198−204.

(10) (a) Becker, J. S.; Zoriy, M. V.; Pickhardt, C.; Palomero-Gallagher, N.; Zilles, K. *Anal. Chem.* **2005**, *77*, 3208−3216. (b) Becker, J. S.; Matusch, A.; Depboylu, C.; Dobrowolska, J.; Zoriy, M. V. *Anal. Chem.* **2007**, *79*, 6074−6080.

(11) (a) Otero-Romaní, J.; Moreda-Piñeiro, A.; Bermejo-Barrera, A.; Bermejo-Barrera, P. *Anal. Chim. Acta* **2005**, *536*, 213−218. (b) Liu, Y.; Liang, P.; Guo, L. *Talanta* **2005**, *68*, 25−30.

(12) (a) Beni, V.; Ogurtsov, V. I.; Bakunin, N. V.; Arrigan, D. W. M.; Hill, M. *Anal. Chim. Acta* **2005**, *552*, 190−200. (b) Ensafi, A. A.; Khayamian, T.; Benvidi, A.; Mirmomtaz, E. *Anal. Chim. Acta* **2006**, *561*, 225−232.

(13) (a) Varnes, A. W.; Dodson, R. B.; Wehry, E. L. *J. Am. Chem. Soc.* **1972**, *94*, 946−950. (b) Kemlo, J. A.; Shepherd, T. M. *Chem. Phys. Lett.* **1977**, *47*, 158−162. (c) Bergonzi, R.; Fabbrizzi, L.; Licchelli, M.; Mangano, C. *Coord. Chem. Rev.* **1998**, *170*, 31−46.

(14) (a) Zheng, Y. J.; Gattás-Asfura, K. M.; Konka, V.; Leblanc, R. M. *Chem. Commun.* **2002**, 2350−2351. (b) Zheng, Y. J.; Orbulescu, J.; Ji, X. J.; Andreopoulos, F. M.; Pham, S. M.; Leblanc, R. M. *J. Am. Chem. Soc.* **2003**, *125*, 2680−2686. (c) Zheng, Y. J.; Cao, X. H.; Orbulescu, J.; Konka, V.; Andreopoulos, F. M.; Pham, S. M.; Leblanc, R. M. *Anal. Chem.* **2003**, *75*, 1706−1712. (d) Li, Y. T.; Yang, C. M. *Chem. Commun.* **2003**, 2884−2885. (e) Mokhir, A.; Kiel, A.; Herten, D.-P.; Kraemer, R. *Inorg. Chem.* **2005**, *44*, 5661−5666. (f) Choi, J. K.; Kim, S. H.; Yoon, J. Y.; Lee, K.-H.; Bartsch, R. A.; Kim, J. S. *J. Org. Chem.* **2006**, *71*, 8011−8015. (g) Mei, Y. J.; Bentley, P. A.; Wang, W. *Tetrahedron Lett.* **2006**, *47*, 2447−2449. (h) Park, S. M.; Kim, M. H.; Choe, J.-I.; No, K. T.; Chang, S.-K. *J. Org. Chem.* **2007**, *72*, 3550−3553. (i) Xie, J.; Ménand, M.; Maisonneuve, S.; Métivier, R. *J. Org. Chem.* **2007**, *72*, 5980−5985. (j) Weng, Y. Q.; Yue, F.; Zhong, Y. R.; Ye, B. H. *Inorg. Chem.* **2007**, *46*, 7749−7755. (k) Quang, D. T.; Jung, H. S.; Yoon, J. H.; Lee, S. Y.; Kim, J. S. *Bull. Korean Chem. Soc.* **2007**, *28*, 682−684. (l) Jung, H. S.; Kwon, P. S.; Lee, J. W.; Kim, J. I.; Hong, C. S.; Kim, J. W.; Yan, S.; Lee, J. Y.; Lee, J. H.; Joo, T.; Kim, J. S. *J. Am. Chem. Soc.* **2009**, *131*, 2008−2012.

(15) (a) Kim, H. N.; Lee, M. H.; Kim, H. J.; Kim, J. S.; Yoon, J. Y. *Chem. Soc. Rev.* **2008**, *37*, 1465−1472. (b) Beija, M.; Afonso, C. A. M.; Martinho, J. M. G. *Chem. Soc. Rev.* **2009**, *38*, 2410−2433. (c) Quang, D. T.; Kim, J. S. *Chem. Rev.* **2010**, *110*, 6280−6301. (d) Chen, X. Q.; Pradhan, T.; Wang, F.; Kim, J. S.; Yoon, J. Y. *Chem. Rev.* **2012**, *112*, 1910−1956. (e) Jeong, Y. S.; Yoon, J. Y. *Inorg. Chim. Acta* **2012**, *381*, 2−14. (f) Culzoni, M. J.; Muñoz de la Peña, A.; Machuca, A.; Goicoechea, H. C.; Babiano, R. *Anal. Methods* **2013**, *5*, 30−49. (g) Zheng, H.; Zhan, X. Q.; Bian, Q. N.; Zhang, X. J. *Chem. Commun.* **2013**, *49*, 429−447. (h) Xiang, Y.; Li, Z. F.; Chen, X. T.; Tong, A. J. *Talanta* **2008**, *74*, 1148−1153. (i) Yang, X. F.; Liu, P.; Wang, L. P.; Zhao, M. L. *J. Fluoresc.* **2008**, *18*, 453−459. (j) Dong, M.; Ma, T. H.; Zhang, A. J.; Dong, Y. M.; Wang, Y. W.; Peng, Y. *Dyes Pigm.* **2010**, *87*, 164−172. (k) Shivaprasad, M.; Govindaraju, T. *Mater. Technol.* **2011**, *26*, 168−172. (l) Tang, L. J.; Guo, J. J.; Wang, N. N. *Bull. Korean Chem. Soc.* **2013**, *34*, 159−163. (m) Zhang, J. G.; Zhang, L.; Wei, Y. L.; Chao, J. B.; Shuang, S. M.; Cai, Z. W.; Dong, C. *Spectrochim. Acta, Part A* **2014**, *132*, 191−197.

(16) (a) Ko, S.-K.; Chen, X. Q.; Yoon, J. Y.; Shin, I. *Chem. Soc. Rev.* **2011**, *40*, 2120−2130. (b) Wang, L.; Yan, J. X.; Qin, W. W.; Liu, W. S.; Wang, R. *Dyes Pigm.* **2012**, *92*, 1083−1090. (c) Yang, Y. M.; Zhao, Q.; Feng, W.; Li, F. Y. *Chem. Rev.* **2013**, *113*, 192−270. (d) Yuan, L.; Lin, W. Y.; Zheng, K. B.; Zhu, S. S. *Acc. Chem. Res.* **2013**, *46*, 1462−1473. (e) Maity, D.; Karthigeyan, D.; Kundu, T. K.; Govindaraju, T. *Sens. Actuators, B* **2013**, *176*, 831−837. (f) Lee, H. Y.; Swamy, K. M. K.; Jung, J. Y.; Kim, G. M.; Yoon, J. Y. *Sens. Actuators, B* **2013**, *182*, 530−537. (g) Jiang, Z. H.; Tian, S. J.; Wei, C. Q.; Ni, T. J. H.; Li, Y.; Dai, L.; Zhang, D. Z. *Sens. Actuators, B* **2013**, *184*, 106−112. (h) Huo, F. J.; Wang, L.; Yin, C. X.; Yang, Y. T.; Tong, H. B.; Chao, J. B.; Zhang, Y. B. *Sens. Actuators, B* **2013**, *188*, 735−740. (i) Adhikari, S.; Ghosh, A.; Mandal, S.; Sengupta, A.; Chattopadhyay, A.; Matalobos, J. S.; Lohar, S.; Das, D. *Dalton Trans.* **2014**, *43*, 7747−7751. (j) Gao, W.; Yang, Y. T.; Huo, F. J.; Yin, C. X.; Xu, M.; Zhang, Y. B.; Chao, J. B.; Jin, S.; Zhang, S. P. *Sens. Actuators, B* **2014**, *193*, 294−300. (k) Puangploy, P.; Smanmoo, S.; Surareungchai, W. *Sens. Actuators, B* **2014**, *193*, 679−686.

(17) (a) Beer, P. D.; Gale, P. A.; Chen, G. Z. *J. Chem. Soc., Dalton Trans.* **1999**, 1897−1909. (b) Staveren, D. R. V.; Metzler-Nolte, N. *Chem. Rev.* **2004**, *104*, 5931−5985. (c) Molina, P.; Tárraga, A.; Caballero, A. *Eur. J. Inorg. Chem.* **2008**, *22*, 3401−3417. (d) Molina, P.; Tárraga, A.; Alfonso, M. *Dalton Trans.* **2014**, *43*, 18−29. (e) Sun, R. L.; Wang, L.; Yu, H. J.; Abdin, Z. U.; Chen, Y. S.; Huang, J.; Tong, R. B. *Organometallics* **2014**, *33*, 4560−4573.

(18) (a) Zapata, F.; Caballero, A.; Espinosa, A.; Tárraga, A.; Molina, P. *Org. Lett.* **2007**, *9*, 2385−2388. (b) Zhang, R. L.; Wang, Z. L.; Wu, Y. S.; Fu, H. B.; Yao, J. N. *Org. Lett.* **2008**, *10*, 3065−3068. (c) Alfonso, M.; Tárraga, A.; Molina, P. *Dalton Trans.* **2010**, *39*, 8637−8645. (d) Alfonso, M.; Espinosa, A.; Tárraga, A.; Molina, P. *Chem. Commun.* **2012**, *48*, 6848−6850. (e) Thakur, A.; Ghosh, S. *Organometallics* **2012**, *31*, 819−826. (f) González, M. D. C.; Otón, F.; Espinosa, A.; Tárraga, A.; Molina, P. *Chem. Commun.* **2013**, *49*, 9633−9635.

(19) (a) Yang, H.; Zhou, Z. G.; Huang, K. W.; Yu, M. X.; Li, F. Y.; Yi, T.; Huang, C. H. *Org. Lett.* **2007**, *9*, 4729−4732. (b) Huang, K. W.; Yang, H.; Zhou, Z. G.; Yu, M. X.; Li, F. Y.; Gao, X.; Yi, T.; Huang, C. H. *Org. Lett.* **2008**, *10*, 2557−2560. (c) Wu, D. Y.; Huang, W.; Lin, Z. H.; Duan, C. Y.; He, C.; Wu, S.; Wang, D. H. *Inorg. Chem.* **2008**, *47*, 7190−7201. (d) Huang, W.; Song, C. X.; He, C.; Lv, G. J.; Hu, X. Y.; Zhu, X.; Duan, C. Y. *Inorg. Chem.* **2009**, *48*, 5061−5072. (e) Arivazhagan, C.; Borthakur, R.; Ghosh, S. *Organometallics* **2015**, *34*, 1147−1155.

(20) (a) Ge, F.; Ye, H.; Luo, J. Z.; Wang, S.; Sun, Y. J.; Zhao, B. X.; Miao, J. Y. *Sens. Actuators, B* **2013**, *181*, 215−220. (b) Mi, Y. S.; Cao, Z.; Chen, Y. T.; Xie, Q. F.; Xu, Y. Y.; Luo, Y. F.; Shi, J. J.; Xiang, J. N. *Analyst* **2013**, *138*, 5274−5280. (c) Cheng, X. W.; Zhou, Y.; Fang, Y.; Rui, Q. Q.; Yao, C. *RSC Adv.* **2015**, *5*, 19465−19469.

DOI: 10.1021/acs.organomet.5b00285
Organometallics 2015, 34, 2962−2970

(21) Xiang, Y.; Tong, A. J.; Jin, P. Y.; Ju, Y. *Org. Lett.* **2006**, *8*, 2863−2866.
(22) Lin, H. C.; Huang, C. C.; Shi, C. H.; Liao, Y. H.; Chen, C. C.; Lin, Y. C.; Liu, Y. H. *Dalton Trans.* **2007**, 781−791.
(23) (a) Connors, K. A. *Binding Constant: The Measurement of Molecular Complex Stability*; John Wiley & Sons: New York, 1987. (b) Valeur, B. *Molecular Fluorescence: Principles and Applications*; Wiley-VCH: New York, 2001.
(24) (a) Shortreed, M.; Kopelman, R.; Kuhn, M.; Hoyland, B. *Anal. Chem.* **1996**, *68*, 1414−1418. (b) Caballero, A.; Martínez, R.; Lloveras, V.; Ratera, I.; Vidal-Gancedo, J.; Wurst, K.; Tárraga, A.; Molina, P.; Veciana, J. *J. Am. Chem. Soc.* **2005**, *127*, 15666−15667. (c) Lin, W. Y.; Yuan, L.; Cao, Z. M.; Feng, Y. M.; Long, L. L. *Chem.—Eur. J.* **2009**, *15*, 5096−5103. (d) Kim, M. H.; Jang, H. H.; Yi, S. J.; Chang, S.-K.; Han, M. S. *Chem. Commun.* **2009**, 4838−4840.
(25) (a) Tchinda, A. J.; Ngameni, E.; Walcarius, A. *Sens. Actuators, B* **2007**, *121*, 113−123. (b) Singh, P. R.; Contractor, A. Q. *Int. J. Environ. Anal. Chem.* **2005**, *85*, 831−835. (c) Crouse, M. M.; Miller, A. E.; Crouse, D. T.; Ikram, A. A. *J. Electrochem. Soc.* **2005**, *152*, D167−D172.
(26) (a) Pandey, R.; Gupta, R. K.; Shahid, M.; Maiti, B.; Misra, A.; Pandey, D. S. *Inorg. Chem.* **2012**, *51*, 298−311. (b) Otón, F.; González, M. D. C.; Espinosa, A.; Tárraga, A.; Molina, P. *Organometallics* **2012**, *31*, 2085−2096. (c) Thakur, A.; Mandal, D.; Ghosh, S. *Anal. Chem.* **2013**, *85*, 1665−1674.
(27) (a) Zapata, F.; Caballero, A.; Espinosa, A.; Tárraga, A.; Molina, P. *J. Org. Chem.* **2008**, *73*, 4034−4044. (b) Shi, L.; Song, W.; Li, Y.; Li, D. W.; Swanick, K. N.; Ding, Z. F.; Long, Y. T. *Talanta* **2011**, *84*, 900−904.
(28) Dujols, V.; Ford, F.; Czarnik, A. W. *J. Am. Chem. Soc.* **1997**, *119*, 7386−7387.
(29) (a) United States Environmental Protection Agency. *Federal Register*, final rule; **1999**, *56*, 26460−26564. (b) Mayr, T.; Klimant, I.; Wolfbeis, O. S.; Werner, T. *Anal. Chim. Acta* **2002**, *462*, 1−10.

DOI: 10.1021/acs.organomet.5b00285
Organometallics 2015, 34, 2962−2970